Science of the Total Environment 894 (2023) 164977

Contents lists available at ScienceDirect

Science of the Total Environment

journal homepage: www.elsevier.com/locate/scitotenv

Transpiration rates decline under limited moisture supply along hillslopes in a humid karst terrain

Wenna Liu [a,b,c], Yunpeng Nie [a,b], Zidong Luo [a,b], Zhongyun Wang [a,b,c], Li Huang [a,b,c], Fei He [b], Hongsong Chen [a,b,*]

[a] Key Laboratory of Agro–ecological Processes in Subtropical Region, Institute of Subtropical Agriculture, Chinese Academy of Sciences, Changsha, Hunan 410125, China
[b] Guangxi Key Laboratory of Karst Ecological Processes and Services, Huanjiang Observation and Research Station for Karst Ecosystems, Chinese Academy of Sciences, Huanjiang, Guangxi 547100, China
[c] University of Chinese Academy of Sciences, Beijing 100039, China

HIGHLIGHTS

- Transpiration pattern along hillslopes can evaluate eco-hydrological functions.
- *R. chinensis* primarily relied on shallow soil water at up and down hillslopes.
- Transpiration rates declined by nearly half to adapt the water-limited environment.

GRAPHICAL ABSTRACT

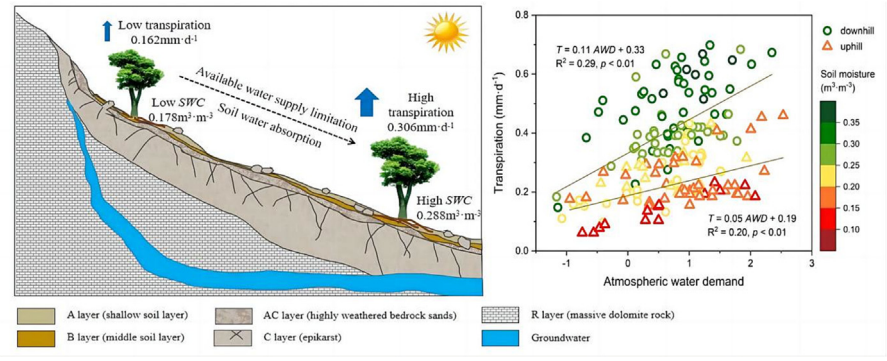

ARTICLE INFO

Editor: Zhaozhong Feng

Keywords:
Transpiration
Plant water source
Water–limitation
Karst ecosystem
Stable isotope

ABSTRACT

Topographic positions can mediate subsurface water availability, but its effects on tree transpiration are controversial. In humid karst regions, climax forests are usually not limited by moisture supply, even at the summit, through absorbing water from deep layers. However, little is known on the transpiration pattern and its limiting factor on the shrubland widely distributed along the karst hillslopes. In the current study, *Rhus chinensis*, a widely spread constructive species in natural restoration was selected. Meteorological factors, 0–300 cm soil–epikarst moisture, sap flow, and root water uptake were studied during an entire growing season to assess how hillslope positions affected transpiration. We found the mean water content in uphill was only around 60 % of that in downhill, indicating a contrasting water supply along the slope. However, there were no significant differences in the xylem isotopic composition and *lc*–excess which suggested the similar water uptake strategies in both uphill and downhill. *R. chinensis* primarily relied on the soil water rather than epikarst water (groundwater) along the hillslope because of the MixSIAR model results and more negative *lc*–excess values (−13.18 ‰). *R. chinensis* exhibited decreases of nearly half in the transpiration rate and amount in uphill compared to those in downhill. In downhill with sufficient water availability, transpiration followed the variation in atmospheric water demand. In uphill, a poor moisture supply limited tree transpiration and its response to atmospheric water demand. Our findings revealed that the early successional species did not entirely depend on atmospheric water demand, absorbing deep epikarst water as the mature forest. The transpiration rates of those species declined by nearly half to adapt to the water–limited environment along the hillslope in the humid karst region. This study can contribute to the evaluation of eco–hydrological functions during natural restoration.

* Corresponding author at: Institute of Subtropical Agriculture, Chinese Academy of Sciences, Changsha, Hunan 410125, China.
E-mail address: hbchs@isa.ac.cn (H. Chen).

http://dx.doi.org/10.1016/j.scitotenv.2023.164977
Received 19 March 2023; Received in revised form 19 May 2023; Accepted 15 June 2023
Available online 20 June 2023

1. Introduction

Transpiration is a dominant determinant of the flux in the water cycle at Earth's critical zone (Jasechko et al., 2013; Schlesinger and Jasechko, 2014; Behzad et al., 2023), impacting vegetation productivity (Gutierrez Lopez et al., 2021), streamflow generation (Vose et al., 2016), and ecosystem services (Yang et al., 2022). Transpiration is usually controlled by atmospheric water demand (*AWD*) and moisture supply (Novick et al., 2016; Jiao et al., 2019; Wu et al., 2021). *AWD* means the original forces of solar radiation and vapor pressure deficit to mediate stomatal opening and closing (Hayat et al., 2020; Deng et al., 2021; Huang et al., 2021). Ecosystem water stress is frequently characterized by low soil water availability limiting transpiration (Clausnitzer et al., 2011; Naithani et al., 2012; Ungar et al., 2013; Dymond et al., 2017; Cai et al., 2018; Liu et al., 2023). Denissen et al. (2022) demonstrated a wide regime shift from ecosystem energy limitation to water limitation under global warming. Topographical factors influence water availability due to the redistribution of soil moisture (Mitchell et al., 2012; Looker et al., 2018; Fan et al., 2019), and this can mitigate or intensify drought effects on vegetation along a hillside gradient (Hawthorne and Miniat, 2017). Differences in forest community composition, tree growth and response to drought have been attributed to topographically driven differences in environmental moisture conditions (Adams et al., 2014; Berdanier and Clark, 2016; Gutierrez Lopez et al., 2021). However, whether the changes in water supply caused by topography can become the dominant factors affecting transpiration remains controversial.

Along a topographic gradient, tree transpiration may vary depending on moisture availability in the subsurface associated with the transpiration limiting factors and water utilization along the slope. Downslope areas are generally understood to have wetter soils than side slopes or ridges (Jencso et al., 2009; Pacific et al., 2011) due to the lateral redistribution of soil moisture, the deeper soil, and the higher water holding capacity (Kumagai et al., 2007; Fan et al., 2019). In arid and semi–arid zones, soil water availability is often the main limiting factor for plant growth. Thus, high soil water availability in downslope areas usually results in a higher rate of transpiration compared to upslope areas (Wang et al., 2017). In humid regions with high annual precipitation, atmospheric water demand is still the main controlling factor for transpiration rather than topographic factors; this causes similar transpiration at upper and lower elevations (Kumagai et al., 2007; Renner et al., 2016; Tsuruta et al., 2020). However, it is uncertain whether the trees may absorb deep water such as groundwater to maintain similar rates of transpiration at upper and lower position on a slope (Dudley et al., 2018; Carrière et al., 2020). Fabiani et al. (2021) observed similar water sources irrespective of hillside position and greater sap velocities at upslope locations in a moderate oceanic climate region; the subsurface hillslope structure promoted vertical water flux over lateral redistribution in the vadose zone. Despite topographic–induced changes in moisture, vegetation in humid regions does not appear to be under water constraint. When the subsurface structure is complex, with rapidly varying hydrological processes along the slope, it is unknown whether plants will show the same transpiration patterns.

The subtropical karst region of southwestern China covers >0.54 million km^2 and is one of the world's largest exposed carbonate rock areas (Yuan et al., 1994). Sufficient heat and moisture have promoted the formation of karst terrain and the development of an intricate network of crevices and cracks in the epikarst (Williams, 1983; Williams, 2008; Zhang et al., 2022). Shallow soil, rapid rainfall infiltration, and a complex underground drainage system move rainwater through cracks and subsurface flow from uphill areas to the depressions (Heilman et al., 2014). Thus, the soil water storage is relatively low along the slope. Within a relatively small distance and variation in altitude, the water storage availability and soil depth decrease sharply from the mesic downhill area to the xeric uphill area (Wang et al., 2020). Previous studies have generally focused on plant transpiration in habitats with relatively deep soil thickness such as the foot of a slope or in a depression (Zhang et al., 2019a; Deng et al., 2021; Wu et al., 2021). All such studies have found that atmospheric water demand is the main influence factor on the transpiration in a subtropical karst region. Huang et al. (2009) and Du et al. (2021) found that transpiration was generally maintained at a high rate (e.g., > 4.0 $mm{\cdot}d^{-1}$ in the growing seasons), even when the shallow layer water content (SLWC, 0–40 cm) dropped to about 0.15 $cm^3{\cdot}cm^{-3}$ during dry spells. They concluded that the plants in this region could take up water from deep layers when the SLWC is limited. However, researchers have usually concentrated on the mature plantations or primeval forest at late stage of succession, and naturally restored secondary forests are rarely investigated.

Large parts of the karst area are covered with restored vegetation in the early stages of succession after ecological engineering employed to combat the rocky desertification and deforestation (North et al., 2009; Jiang et al., 2014). The early successional plant communities were usually more dependent on recent rainwater received within short time spans (Nie et al., 2018; Luo et al., 2023). Previous studies have indicated that most of the fine roots of woody species in shallow rocky soil habitats are concentrated in the upper 20 cm soil depth in karst ecosystems, and these roots accounted for >57 % of root biomass and decreased with increasing soil depth (Du et al., 2019; Huang et al., 2022). *Rhus chinensis*, a typical constructive species in early successional communities, is widely distributed along the hillsides of karst areas (Yin, 2011; Devi and Singh, 2018). Previous studies have shown that *R. chinensis* is a pioneer woody species characterized by strong adaptability, rapid growth, and high root tillering ability (Zhou et al., 2017). Our field investigations have suggested that *R. chinensis* could easily be uprooted, indicating its shallow root distribution. The small sapwood area of *R. chinensis* indicates that it is easily affected by drought (Fig. S1). *R. chinensis* trees are generally smaller in size at higher positions on the slope compared to lower elevations, presumably due to the slow growth rate with low transpiration needed to adapt to the drought stress. Therefore, describing the transpiration patterns and how they are influenced by atmospheric water demand and moisture supply of constructive species are important factors that need to be evaluated for understanding eco–hydrological functions and constructing dynamic vegetation models.

The current study monitored several environmental factors affecting the early natural restoration of *R. chinensis* during the growing season: meteorological factors and variation in the water content in 0–300 cm karst critical zone at different topographic positions, the sap flow and the water uptake depth., The analysis considered the transpiration patterns, and its limiting factors along the hillslope. We hypothesized that: (1) *R. chinensis* would rely on the shallow soil water no matter whether in a at sufficient moisture environment lower down the slope or in a water–limited environment higher up the slope; (2) *R. chinensis* would be affected by atmospheric water demand and moisture supply and would exhibit lower transpiration higher up the slope. The main objectives of the study were: (1) to explore root water sources and transpiration patterns of *R. chinensis* at different topographic positions; (2) to examine the effects of atmospheric water demand and moisture supply on transpiration.

2. Materials and methods

2.1. Study site description

The study site was located in a small catchment (area = 1.14 km^2, altitude from 252 to 500 m) in the Huanjiang Observation and Research Station for Karst Ecosystems of the Chinese Academy of Sciences (24°43′58.9″–24°44′48.8″N, 108°18′56.9″–108°19′58.4″E), situated in northwest of Guangxi Province, China. The watershed is a typical karstic peak–cluster depression area with a flat depression (area = 22.1 hm^2) surrounded by mountain ranges on three sides and the mouth of the watershed in the northeast. Approximately 60 % of the hillsides land have a slope >25°. The loose rocky soils usually consist of a thin layer of coarse gravel underlain by a thick layer of soil and rock fragments, with a depth of around 60 cm along the slope. Soils are well–drained, gravelly, and calcareous, with stable infiltration rates ranging from 40 to 130 $mm{\cdot}h^{-1}$. The epikarst has a near–steady infiltration rate of approximately 35 $mm{\cdot}h^{-1}$, where the subsurface runoff occurs along the soil–epikarst interface and is dominated

by preferential flow. Large amounts of soil material are deposited at the foot of the slope and depression with surface runoff and erosion from the hillslope during heavy rainstorms (Wang et al., 2019). Thus, within a relatively small distance and variation in altitude, water storage availability and soil depth decrease steeply from the mesic downhill areas to the xeric uphill areas along karst slopes. There are two springs and a stream in the catchment. The springs are at the bases of hillssides; the first one is an intermittent spring that flows during the wet season and the second one is a perennial spring. The region has a subtropical mountainous monsoon climate, with mean annual precipitation of 1389.1 mm and an annual temperature of 18.5 °C. The wet season lasts from late April to the end of September and provides >60 % of the total annual rainfall. The pronounced six–month dry season in winter/spring provides 20–30 % of the annual rainfall.

This area experienced severe deforestation from 1958 to the mid–1980s and has been under natural restoration for almost 25 years (Tong et al., 2018). The distribution pattern of plant communities was formed as grass and shrub at upper elevations and secondary forest lower down the slope under long–term natural vegetation recovery (Nie et al., 2019; Meng et al., 2022). To explore plant transpiration and its response pattern along the slope, two sample plots were selected at uphill and downhill (Fig. 1). In the uphill plot, *R. chinensis* as the only tree species dominated the overstory tree layer. *Dicranopteris linearis* dominated the herbaceous layer. In the downhill plot, *Rhus chinensis*, *Mallotus philippensis*, *Vitex negundo* and *Pyracantha fortuneana* were the dominant species. Although the species diversity was high, *R. chinensis* was in the top three in importance value in the overstory tree layer. In the growing season, the leaves regrow around in the middle of March, reach peak growth in June, and fall off in October. Other information concerning the sampling plots is listed in Table 1.

2.2. Transpiration measurement

Sap flux (*SF*) of *R. chinensis* in the two plots was monitored using a Thermal Dissipation Probe (TDP, FLGS – TDP XM1000 connected to a CR1000 datalogger, USA) as described by Granier (1987) during the full growing season from the day of year (*DOY*) 60 to 304 (1st March 2021 to 31st October 2021). According to the species DBH distribution, four TDPs were installed in each plot (Table 2). In a previous field investigation, we found that *R. chinensis* generally showed a thin sapwood depth but a thick heartwood depth (Fig. S1). The average sapwood depth was 8.16 ± 2.96 mm (N = 14 the ranges of DBH from 4.5 cm to 10 cm). Thus, we chose 10 mm–long probes with the heating point in the middle (5 mm) to coincide with the sapwood depth. The probes were 1.2 mm in diameter, with a probe interval of 40 mm. All the TDPs were inserted into the sapwood of stems 1.3 m above ground and on the north sides of the trunks. The upper probe was heated with a constant direct current, while the lower probe remained at trunk temperature (the reference probe). Each probe contained a copper – Constantan thermocouple positioned half way along its length. Both thermocouples were connected to yield a temperature difference between the two probes. The temperature difference data were measured automatically every 10 min. Sap flow density (J_s, $g{\cdot}H_2O{\cdot}s^{-1}{\cdot}m^{-2}$) was calculated as follows:

$$J_s = 119 \times [(\Delta T_{max} - \Delta T)/\Delta T]^{1.231} \quad (1)$$

where ΔT is the temperature difference between the two probes, and ΔT_{max} is the maximum value of ΔT recorded at the no–transpiration state when J_s is zero.

The daily sap flux (SF, $m^3{\cdot}m^{-2}{\cdot}d^{-1}$) was calculated as follows:

$$SF = \left(\sum_{i=1}^{n=144} J_s \times 60 \times 10\right)/10^6 \quad (2)$$

where 60 means 60 s and 10 means 10 min. The sap flow flux in 10 min was calculated by multiplying *Js* (sap flow density per second) and time (60 s × 10 min).

The daily transpiration rate (T, $mm{\cdot}d^{-1}$) was calculated as follows:

$$T = \frac{SF \times A_s}{A_c} \times 10^3 \quad (3)$$

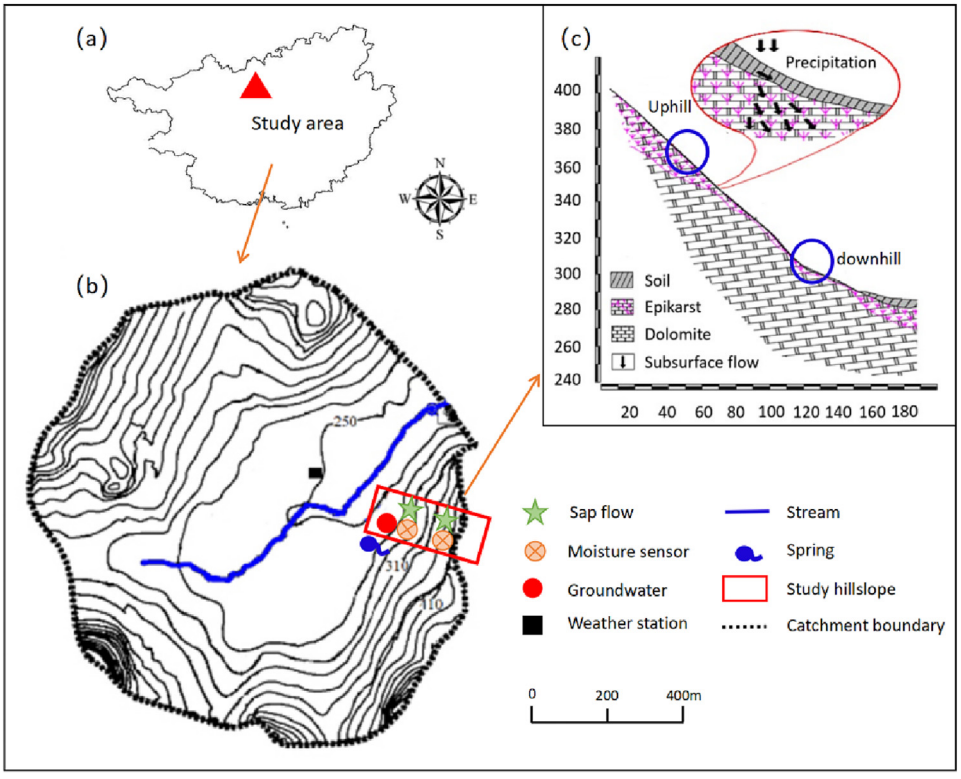

Fig. 1. (a) Location of the study area in Guangxi Province, China; (b) topographic map of the study area and sites for sap flow and moisture measurement along the hillslope; (c) schematic diagram profile line for geological inference of the study hillslope.

Table 1
The information of sample plots.

Slope position	Elevation (m)	Gradient	Gravel content (%)	Organic content (g/kg)	Soil thickness (cm)	High-weathered bedrock thickness (cm)	Vegetation type	Vegetation coverage
Uphill	348.16	47°	23.19	50.01	40	20	Grass-shrub	90 %
Downhill	263.38	26°	43.86	62.29	50	30	Second forest	85 %

where A_s is sapwood area, and A_c is canopy area of each tree, as shown in Table 2.

2.3. Environmental factor measurements

Soil water content in various layers was continuously monitored by FDR probes through excavating sections according to the soil generation layer at 0–20, 20–40, and 40–60 cm depth in the uphill plot and at 0–20, 20–50, and 50–80 cm depth in the downhill plot. Among these, 0–20 cm was the A horizon, i.e., the shallow soil layer; 20–40 cm in the uphill plot and 20–50 cm in the downhill plot was the B horizon, i.e., middle soil layers; and 40–60 cm in the uphill plot and 50–80 cm in the downhill plot was the AC layer, i.e., highly weathered bedrock sands (deep soil layer). Soil moisture sensors were installed at two randomly chosen points in each plot. Although there were only two points for continuous measurement, the results were reliable. Zhang et al. (2023) collected continuous data of soil water content for long–term (about nine years) measurement, and the results strongly supported our measurements. In addition, except for the continuous monitoring of soil moisture by using FDR probes, a single gravimetric soil water content measurement was also performed by collecting soil samples simultaneously with soil water isotopic analysis. These soil samples were obtained from six/seven depth intervals (0–10, 10–20, 20–30, 30–40, 40–50, 50–60, and 60–80 (only in the downhill plot) with an auger and five replicates were collected from each layer.

Epikarst water content was monitored by FDR probes at 60–120 (uphill)/80–120 (downhill), 120–180, 180–240, and 240–300 cm at three-meter-deep boreholes in the uphill and downhill plots in karst critical zone platforms. The details concerning measurements can be found in Zhang et al. (2022). All the probes were calibrated according to Yang et al. (2019). The overall soil water content (*SWC*, $m^3 \cdot m^{-3}$) was calculated using the arithmetic weighted average as follows:

$$SWC = \Sigma_{i=1}^{n=3} \theta_i \times h_i \quad (4)$$

where θ_i is the soil water content of the i_{th} layer, and h_i is soil thickness of the i_{th} layer.

Meteorological data, including temperature (*T*, °C), relative humid (*RH*, %), solar radiation (R_s, $MJ \cdot m^{-2}$) and precipitation (*P*, mm) were collected at a meteorological station located in the middle of the same small catchment. Vapor pressure deficit (*VPD*, kPa) was calculated as follows:

$$VPD = 0.611e^{[17.502T/(T+240.97)]}(1 - RH) \quad (5)$$

Table 2
The characteristic of *Rhus chinensis*.

Slope position	Number	DBH (cm)	Height (m)	Canopy area (m × m)	Sapwood area (m^2)	Age
Uphill	1	5.6	4.5	2.3 × 2.5	0.0013	18
	2	5.3	4.8	2.8 × 2.2	0.0011	15
	3	5.8	5.2	2.1 × 2.5	0.0013	16
	4	7.1	5.3	3.3 × 2.8	0.0015	20
Downhill	1	7.2	7.7	3.3 × 2.8	0.0016	19
	2	8.5	7.2	3.2 × 2.5	0.0023	21
	3	7.4	7.5	4 × 4.5	0.0017	18
	4	7.6	7.8	4.4 × 3.5	0.0018	19

2.4. Sampling and stable isotope analysis

Rainwater samples were routinely collected for each rain event above 5 mm from 1st March 2021 to 31st October 2021. Groundwater was sampled from an 11 m borehole around 5 m away from the downhill sample plot once a week regularly during the study period and was collected at the same time as plant and soil sampling. The isotopic composition of groundwater was not enriched by evaporation, and was used to represent epikarst water. All water samples were stored in cap vials, wrapped in parafilm and stored in a freezer until the analysis of stable isotopes was performed.

Xylem and soil samples were taken six times (*DOY* 76, 121, 169, 190, 227, and 286, corresponding to March 17th, May 1st, June 18th, July 9th, August 15th, and October 13th) during the growing season. We selected four individuals as replicates in each plot. Shoots ranging from 0.3 to 0.5 cm in diameter and 3 to 5 cm in length were collected at midday from stems more than two years old; the outer bark and phloem of the shoots were removed to obtain the xylem samples. Soil samples were obtained from six / seven depth intervals (0–10, 10–20, 20–30, 30–40, 40–50, 50–60, and 60–80 (the latter only in the downhill plot) with an auger and five replicates were collected at each layer. The xylem and soil samples were stored at −20 °C for isotopic analysis.

The xylem and soil samples were extracted by a cryogenic vacuum distillation system (LI–2100, LICA, Beijing, China). The isotopic composition of xylem and soil water samples was measured using liquid water isotope ratio infrared spectroscopy (IRIS, DLT–100, Los Gatos Research, Mountain View, CA, USA) at the Key Laboratory for Agro–ecological Processes in Subtropical Region, Chinese Academy of Sciences. The isotope composition is reported in δ notation relative to V–SMOW as

$$\delta^2H\ (\delta^{18}O) = (R_{sample}/R_{standard} - 1) \times 10^3 \quad (6)$$

where R_{sample} and $R_{standard}$ are the ratio D/H or $^{18}O/^{16}O$ of a measured sample and a standard sample, respectively. The standard deviations for repeated measurements were ±1 ‰ for δD and ±0.2 ‰ for $\delta^{18}O$.

Extracting water from plant xylem using cryogenic vacuum distillation can mix organic materials (e.g., methanol and ethanol) that may affect the spectroscopy and lead to erroneous stable isotope values when analyzing with IRIS (Schultz et al., 2011; Wu et al., 2019). An error correction formula was established in our previous study in order to remove the effects pollution of methanol and ethanol (Liu et al., 2021).

We calculated the line-conditioned excess (*lc*-excess) values of xylem water following Landwehr and Coplen (2006). The *lc*-excess values were used to identify the offset of environmental waters from precipitation. A negative *lc*-excess that exceeds the standard deviation of the local meteoric water line (LMWL) indicates that the water has undergone evaporative isotopic enrichment (Evaristo et al., 2015). The *lc*-excess values of the samples were calculated as follows:

$$lc - \text{excess} = \delta^2H - a\,\delta^{18}O - b \quad (7)$$

where the subscript a and b are the slope and intercept of the LMWL, respectively. The LMWL showed the relationship between δ^2H and $\delta^{18}O$ in precipitation: $\delta^2H = 8.37\delta^{18}O + 14.45$, $R^2 = 0.95$, $p < 0.001$.

2.5. Data analysis

Plant water source partitioning was determined by the Bayesian mixing model MixSIAR (version 3.1.7). The raw isotopic ratios of the xylem water

were input into MixSIAR as mixture data. The averages and standard deviations of the different depths of soil water and groundwater were the source data. The discrimination was set to zero for both δ^2H and $\delta^{18}O$ because there is generally no isotopic discrimination of water during plant uptake by roots. For the subsequent analysis and comparison, the plant water sources were divided into shallow (0–20 cm), middle (20–40 cm uphill and 20–50 cm downhill), and deep (40–60 cm uphill and 50–80 cm downhill) soil layers and groundwater according to the fluctuations and patterns of isotopic ratios, the impact of rainfall pulses, and soil water content. (1) The 0–20 cm: this layer was the A horizon, with large fluctuations in soil water content and isotopic composition due to rainfall pulses and evaporation with seasons. (2) The 20–40 cm layer (uphill) and 20–50 cm layer (downhill): this layer was the B horizon, with high clay content and soil bulk density. The vertical recharge of rainfall was difficult to pass through the clay to infiltrate the deeper layer. The variability of soil water isotopic composition and soil water content in this layer were less than that of the 0–20 cm soil layer. (3) The 40–60 cm (uphill) and 50–80 cm (downhill) layer: this layer was the AC horizon, occurring in surface carbonate rocks between the heavy clay soil and hard bedrock. Water was recharged by the preferential flow on the slope, and its isotopic values were close to those of recent rainfall. Water content decreased rapidly after several days of rain.

Statistical analysis was performed with SPSS 17.0 software (SPSS, Chicago, IL, USA). One–way ANOVA and independent samples t–tests were used to detect significant differences. A critical value of $p < 0.05$ was used to identify statistical significance. Partial correlation was used to analyze the relationship between environmental factors and transpiration. Principal component analysis (PAC) was used to reduce the dimension of environmental factors that affected transpiration. The factor scores (possibly negative numbers) after the PAC were saved as the comprehensive factors and further used to regress with transpiration. The figures were plotted with Origin software version 9.0 (Origin, Origin Lab, Farmington, ME, USA).

3. Results

3.1. Variation of environmental factors over the growing season

Precipitation was concentrated in April to August, and the cumulative precipitation was 917.8 mm during the study period (Fig. 2a). *RH* maintained high values from March to May, a result that was related to the many light rainy days and fewer sunny days. *RH* was below 80 % from June to October with mild fluctuations (Fig. 2a). *T*, *VPD*, and R_s showed similar variation patterns during the study period (Fig. 2b). All three meteorological factors increased starting from March and kept high values during June to September, then declined significantly in October.

The mean water content was lower in the uphill plot (19.35 % in soil and 10.08 % in epikarst) than that in the downhill plot (30.94 % in the soil and 19.26 % in the epikarst) (Fig. 3a, c). The moisture response to rainfall differed between the two slope positions. In the uphill plot, the water content increased due to the infiltration of precipitation and then rapidly declined, especially when there was no precipitation for several days in June (Fig. 3b), indicating the poor water storage capacity of the soil. The epikarst water content in the 120–180 cm layer was as high as that in topsoil after heavy rainfall, indicating the preferential flow among cracks in the epikarst (Fig. 3b). In the downhill plot, lateral flow was also an important driver of water recharging, resulting in the relatively high moisture level, even when there was no precipitation for several days in June (Fig. 3d). The variation in water content variation in the epikarst was not consistent with the pattern of precipitation, indicating that there was no rainfall recharging for these depth due to the rock structure.

3.2. Isotopic composition and root water sources

The isotopic composition of xylem water varied significantly ($p < 0.01$) and gradually became more negative with the progress of the season (Fig. 4). The *lc*–excess was less negative from March to October. No significant differences ($p > 0.05$) in xylem water isotopic composition or *lc*–excess occurred between the uphill and downhill plots except in June and July. The xylem water from both uphill and downhill plots showed below the LMWL and overlapped with soil water in the dual–isotope space (Fig. S2).

According to the MixSIAR results, *R. chinensis* primarily absorbed the soil water rather than the groundwater during the growing season at the two sites (Fig. 5). In the uphill plot, the water in the shallow and middle soil layers was the main water source for the trees, except in June. At the downhill sites, *R. chinensis* relied on shallow soil layer water, except in June. In June, *R. chinensis* exhibited the highest transpiration rate corresponding to the increase water uptake from middle and deep layers in the uphill and downhill plots, respectively.

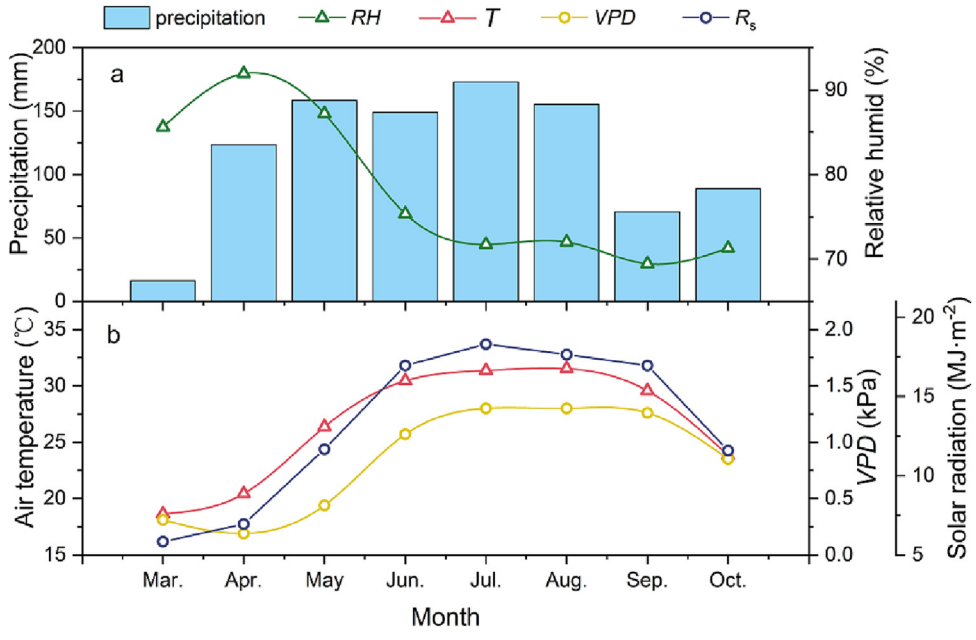

Fig. 2. Monthly variation of (a) precipitation *P* and relative humidity *RH*, (b) temperature *T*, vapor pressure deficit *VPD*, and solar radiation R_s over the growing season.

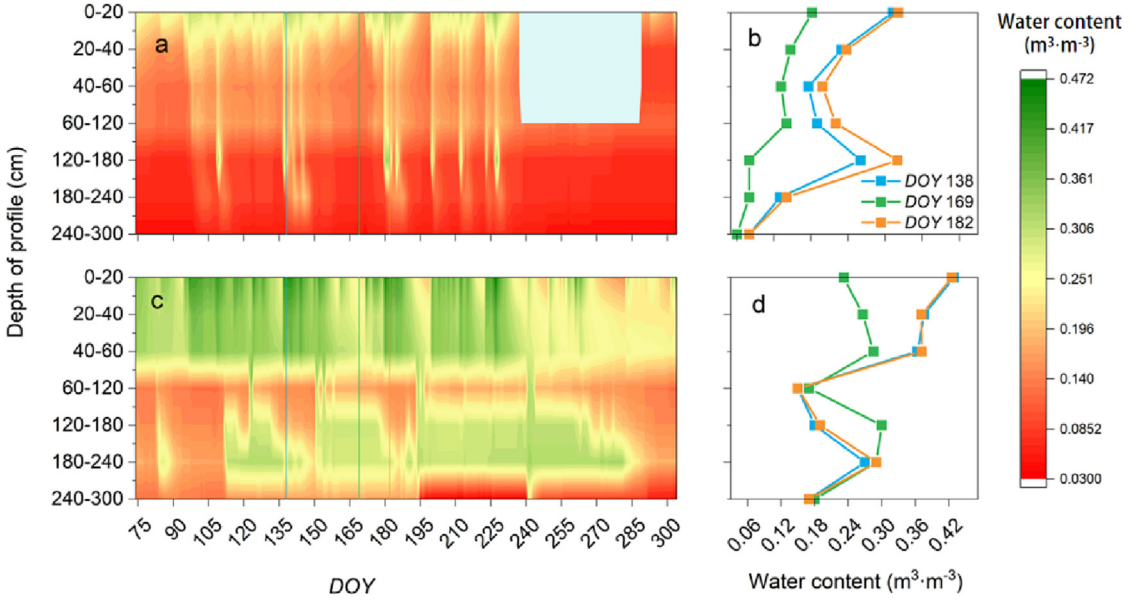

Fig. 3. Daily variation of soil–epikarst water content (a) in the uphill plot during the growing season (the soil moisture data (0–60 cm depths) were lost during 27 August to14 October 2021 as shown in gray), (b) in the uphill along the profile on DOY 138 (55.2 mm of precipitation on DOY 137), DOY 169 (13 continuous sunny days before that day), DOY 182 (52.4 mm of precipitation on DOY 181); (c) in the downhill plot during the growing season; (d) in the downhill plot along the profile on DOY 138 (55.2 mm of precipitation on DOY 137), DOY 169 (13 continuous sunny days before that day), DOY 182 (52.4 mm of precipitation on DOY 181).

3.3. Variation of daily transpiration and its response to environmental factors

The daily transpiration exhibited significant variation in temporal and position scales (Fig. 6). At the temporal scale, *T* increased with the leaf emergence (approx. 13th–19th March), reached the maximum values in June, then gradually decreased. Compared to downhill, the transpiration rate was significantly lower ($p < 0.05$) in the uphill plot. Daily transpiration decreased by nearly half in the uphill plot (0.162 mm·d^{-1}) compared to the downhill plot (0.306 mm·d^{-1}) except in March. The total transpiration amount during the entire growing season showed the same characteristics.

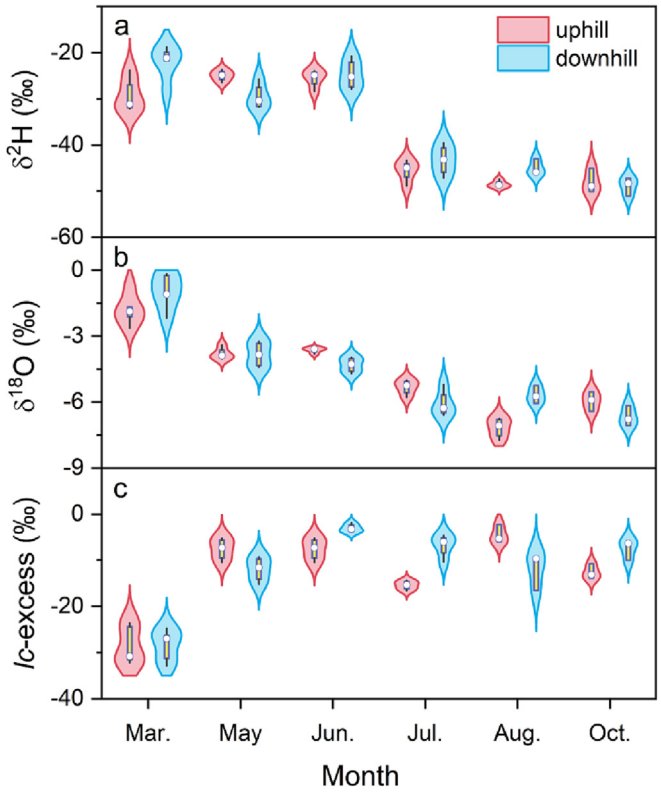

Fig. 4. (a) δ^2H, (b) δ^{18}O, and (c) *lc*–excess of xylem water for each sampling campaign across the growing season. The center line in the boxplot indicates the median, and the lower and upper extremes indicate the first and third quartiles, respectively. The whiskers indicate points within 1.5 times the interquartile range above or below the median.

Partial correlation analysis showed that transpiration was significantly positively correlated with precipitation, temperature, solar radiation, vapor pressure deficit and soil water content in the 0–60 cm layer ($p < 0.05$, Table S1). The epikarst water content showed no significant correlation with *T* ($p > 0.05$, Table S1). Principal component analysis reduced the dimension of correlated environmental factors to two categories as atmospheric water demand (*T*, *RH*, R_s, *VPD*) and soil water content (V_1, V_2, V_3), together explaining 75.86 % (in the uphill plot) and 79.11 % (in the downhill plot) of the variance in transpiration (Fig. S3).

Transpiration showed significant ($p < 0.01$) positive correlations with atmospheric water demand (*AWD*) at the two topographic positions (Fig. 7). The slope of the regression line for the uphill plot was nearly half that of the regression line slope for the downhill plot, indicating the low response of transpiration to *AWD* at higher elevations. In addition, transpiration decreased with the soil moisture decrease. In other words, under similar *AWD* conditions, transpiration depended on the soil moisture supply, resulting in lower transpiration at the higher elevation than that at the lower elevation.

4. Discussion

4.1. Contrasting water content along the hillslope

The water environment was significantly different at the two topographic positions in our study. The mean water content was 0.178m^3·m^{-3} in the uphill plot, approximately 60 % of that at the lower elevation, indicating a large water available supply difference along the slope. These results were consistent with previous studies (Mohanty and Mousli, 2000; Zhang et al., 2019c). Xu et al. (2020) advised separating hillslopes and depressions into two hydrological response units when studying eco–hydrological process in karst regions. Large differences in soil–rocky structure, including soil distribution, rock exposure, and the development of underground matrices and conduits, will resulte in different

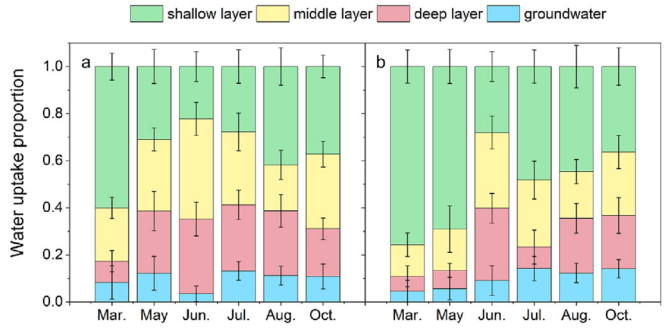

Fig. 5. The water use proportion (a, uphill and b, downhill) of different layers across the growing season.

hydrological processes and water content along the slopes (Chen et al., 2017; Zhang et al., 2019b).

In uphill, soil layers showed poor water holding capacity with a large osmotic coefficient (Meng et al., 2022). Epikarst layers developed large pipes and cracks (Zhang et al., 2022), and were easily to generate a preferential flow transiently during and within two days after a rain. After a period of time without precipitation (five to seven days), the water content decreased along the profile (Yang et al., 2019). In downhill, the soil usually showed a high water holding capacity related to the soil thickness and soil properties. Soil thickness, especially the clay layer with high soil bulk density (nearly 1.55), increased lower down the slope. Meanwhile, impervious layers prevented the precipitation and soil water from achieving vertical infiltration. Fu et al. (2015) indicated that 15 % to 45 % of rainfall was partitioned into subsurface flow on hillslopes and then flowed to depressions during simulated rainfall experiments. The infiltration of rainwater from up–slope to down–slope was altered by vertical flow to lateral flow that was connected through the soil–epikarst interface and finally converged in the low–lying area (Zhang et al., 2022). Springs could also recharge the epikarst layer in the wet season (Wang et al., 2020). Therefore, multiple–sources recharge and high water holding capacity promoted the high moisture at the lower elevation.

4.2. Similar root water uptake strategies at two topographic positions

Xylem isotopic composition varied seasonally but was consistent in the two topographic positions, suggesting that at our study site, trees largely relied on soil water rather than groundwater. Previous studies have found that unlike the deep penetration of root in arid karst region (Schwinning, 2010; Ellsworth and Sternberg, 2015), the root system was dominated by horizontal extension and concentrated in the surface soil layer in dolomite subtropical karst region (Nie et al., 2014; Du et al., 2019; Liu et al., 2019; Ma et al., 2020). Huang et al. (2022) found that a large amount of fine root biomass was concentrated in the shallow soil layer on hillslopes in our study area. In our study, we found that the coarse root system of *R. chinensis* exhibited large radial extension (>3 m) within 40 cm depth (Fig. S4). The roots were difficult to penetrate the hard bedrock for groundwater absorption. Meanwhile, the *lc*–excess of xylem water was more negative, indicating that the species might use water sources with enriched in heavy isotopes due to evaporation (Gaj et al., 2015; Juhlke et al., 2021). Previous studies have found that the dominant species utilized water from surface soil horizons during the growing season in subtropical karst regions (Liu et al., 2021; Yan et al., 2022; Zeng et al., 2021). When sufficient water was available to the plants, especially at the foot of the slope, plants tended to obtain water through the shallow soil layers and consumed large amounts of water.

In uphill, *R. chinensis* still mainly absorbed water from the shallow soil layers and kept a low transpiration rate as an adaptation to the water–limited environment. Previous studies suggested that the low plant transpiration rates were primarily associated with the deep–water sources during drought in karst regions (Wu et al., 2021). Water shortages in deep bedrock at higher elevations decreased the availability of water from deeper layers. In our study, the mean water content in the epikarst was lower (10.08 %) than that in soil (19.35 %) in the uphill plot. The vegetation community features herbs with scattered shrubs and is controlled by soil–type related soil properties, indicating a water–limited environment (Meng et al., 2022). In addition, the competition for resources is strong in the early states of succession in humid regions. Species prefers to occupy more aboveground resources for growth rather than developing deep–rooted systems for water. Therefore, despite soil water content exhibiting a significant difference

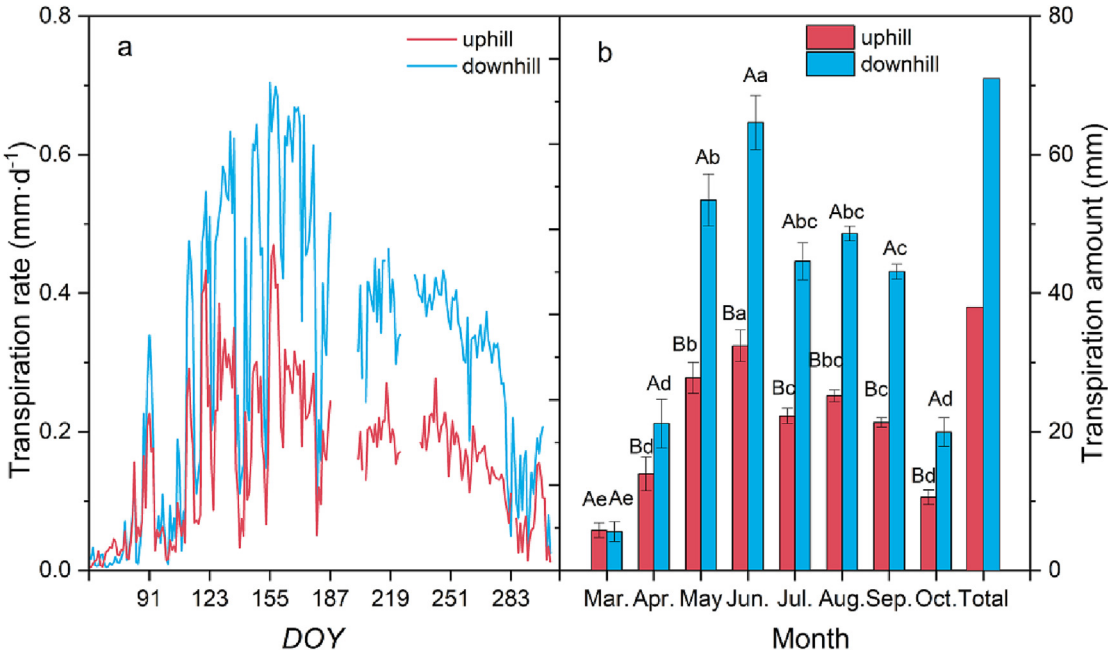

Fig. 6. (a) Seasonal changes of daily transpiration (T, mm·d^{-1}, average of four sampled trees) in the uphill and downhill sites. (b) Average daily transpiration in different months and the total transpiration amount during the growing season. Capital letters indicate significant differences between uphill and downhill plots at the 0.05 level; lowercase letters indicate significant differences among months at the 0.05 level.

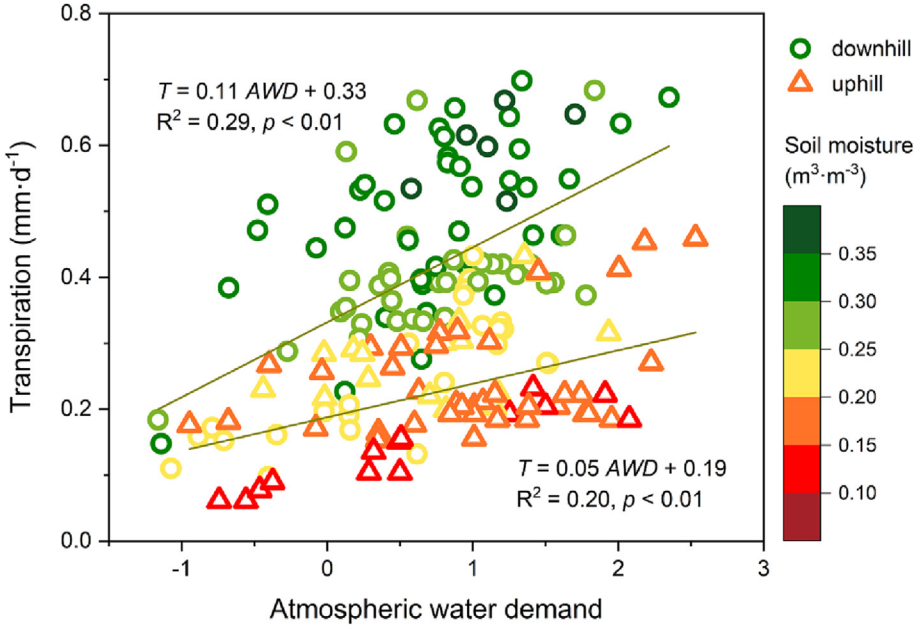

Fig. 7. Regression of transpiration and atmospheric water demand with the variation of soil moisture. Regression lines, regression formulas, explained variance (R^2) and significance (p value) of the linear models for the uphill and downhill plots are shown.

between topographic positions, *R. chinensis* exhibited no significant water source segregation, primarily utilizing soil water. This water uptake pattern explained why *R. chinensis* was easily uprooted and grew slowly and was prone to suffer drought in the uphill site but grew well lower down. In the thin soil of rocky mountain regions in northern China, Liu et al. (2022) also found that the water sources utilized by *Pinus tabuliformis* exhibited no variation with elevation or growing stage. The similar water use patterns along the hillslopes may be the result of long–term adaptation to environmental conditions. Thus, the similar root uptake strategies for shallow soil water supported our first hypothesis. The low sensitivity of water uptake patterns to the hillslope position suggested poor adaptation to environmental changes, especially under climate change scenarios, and greater dependence on the root zone moisture.

R. chinensis usually tended to transpire water supplied by the shallow layer, but when the transpiration rate was the highest in June, the tree increased the absorption ratios from middle and deep soil layers. Tall trees could utilize deeper and more stable soil water to maintain the high transpiration demand when the shallow soil moisture was insufficient (Huang et al., 2009; Du et al., 2021). In our study, the shallow soil water content declined in June (0.32 $m^3 \cdot m^{-3}$) compared to May (0.36 $m^3 \cdot m^{-3}$). Along the soil profile, evaporation occurred in the shallow layers, leading to the decrease of soil potential compared to deeper layers (Song et al., 2009). Zunzunegui et al. (2018) demonstrated that most plants show a preference for easily accessible water under limited water availability. Therefore, the roots were inclined to absorb soil water from deeper layers and switched water use strategies under high transpiration demand.

4.3. Water supply limitation influenced transpiration patterns along the hillslope

R. chinensis exhibited decreases in transpiration rate and total amount during the growing season in the uphill plot, nearly half of the rate and amount compared to the downhill plot, suggesting a distinct transpiration pattern along karst hillslopes in humid areas. Generally, in humid regions plant transpiration is dominated by atmospheric water demand rather than soil water (Oogathoo et al., 2020; Zeng et al., 2021; Wang and Zheng, 2022). Kumagai et al. (2007) and Loranty et al. (2008) found no significant correlation between soil moisture and sap flux, which caused the similar transpiration rates at upper and lower plots during the growing season. In karst depression habitat with sufficient moisture, Zhang et al. (2019a) also concluded that *VPD* and *PAR* were the primary factors controlling the transpiration and that soil moisture had no significant correlation with transpiration. Along the slope, Renner et al. (2016) found that solar radiation was a dominant factor for transpiration, although topographic factors could enhance the response of transpiration to soil water limitation during dry summer periods.

In our study, atmospheric water demand as a main driver also exhibited significant correlations with transpiration at the two topographic positions. The slope value of the regression formula for the uphill plot was half of that for the downhill plot, indicating that the sensitivity of transpiration to *AWD* was also affected by soil water content. Huang et al. (2009) found that *VPD* (rather than *SWC*) was more important in influencing transpiration under sufficient soil moisture conditions. Under seasonal drought conditions, the contribution of atmospheric *VPD* limitation to plant transpiration was decreased, and soil moisture limitation was increased (Song et al., 2020). But Bovard et al. (2005) thought that low soil water content generally resulted in increased stomatal sensitivity to increasing *VPD*. The reason that caused diverse responses of transpiration to *AWD* under low soil moisture was the different first limiting factors for transpiration, i. e. water supply or atmospheric water demand (Loranty et al., 2008). In our study, water supply was the first limiting factor, as it caused a decrease by nearly half in transpiration under similar atmospheric water demand at uphill and downhill positions.

Soil water content showed a significant positive correlation with transpiration in our study, a result that was consistent with previous studies in subalpine catchment (Nathaniel et al., 2018), and in arid (Pei et al., 2019) and semi–arid (Wang et al., 2017) areas. In semi–arid regions, soil water supply for vegetation was relatively low and was influenced by topographic position, resulting in a higher transpiration rate at the foot of the slope than that at higher elevations (Wang et al., 2017). Gessler et al. (2022) found that during the drought period, transpiration was (1) decoupled from *VPD* and primarily governed by soil moisture and (2) declined by a factor of 2.3 compared to pre–drought conditions. In our study, the drought was shifted from the temporal scale to the spatial scale. We also found similar results as in Gessler et al. (2022), and our results supported the second hypothesis. The contrasting differences in soil moisture along the slope influenced and limited plant transpiration, results that highlighted the impact of moisture supply caused by topographic positions in humid karst regions.

5. Conclusion

Patterns of transpiration and its limiting factors in the early successional constructive species at two topographic positions in a subtropical karst critical zone were examined by analyzing environmental variables and root water uptake strategies. We found that the transpiration rate showed a single peak trend during the growing season at the two topographic positions, reaching a peak in June. *R. chinensis* exhibited decreases in transpiration rate and amount by nearly half in the growing season at an uphill site compared to a downhill site, largely due to the soil water supply. *R. chinensis* primarily relied on the soil water along the hillslope, as indicated by the seasonal fluctuation in xylem isotopic composition and more negative *lc*–excess, with no significant difference between uphill and downhill areas. The soil moisture showed high values from April to August at the two positions. However, the mean soil water content in the uphill plot (19.35 %) was only around 60 % of that in the downhill plot (30.94 %) in the entire growing season, indicating the contrast in water supply along the slope. At the downhill site with sufficient water availability, transpiration followed the variation in atmospheric water demand (*AWD*). At the uphill site, the poor moisture supply limited tree transpiration and its response to atmospheric water demand (about half of the slope value of the *AWD*–*T* regression equation for the downhill plot). Our findings revealed that transpiration by the early successional naturally restored species declined by nearly half to adapt to the water–limited environment along the hillslope in the humid karst region, serving for the evaluation of eco–hydrological functions of natural restoration in southwest China. Further studies should account for the response of the stomatal regulation and hydraulic functions on transpiration in order to evaluate vegetation restoration efforts in the face of future climate change.

Funding

This study was supported by the National Natural Science Foundation of China (41930866, 42107103) and Outstanding Member of the Youth Innovation Promotion Association of the Chinese Academy of Sciences, China [Y2022095].

Data availability

Data will be made available on request.

Declaration of competing interest

The authors declare that they have no known competing financial interests or personal relationships that could have appeared to influence the work reported in this paper.

Appendix A. Supplementary data

Supplementary data to this article can be found online at https://doi.org/10.1016/j.scitotenv.2023.164977.

References

Adams, H.R., Barnard, H.R., Loomis, A.K., 2014. Topography alters tree growthclimate relationships in a semi–arid forested catchment. Ecosphere. 5 (11), 1–16.

Behzad, H.M., Arif, M., Duan, S., Kavousi, A., Cao, M., Liu, J., Jiang, Y., 2023. Seasonal variations in water uptake and transpiration for plants in a karst critical zone in China. Sci. Total Environ. 860, 160424.

Berdanier, A.B., Clark, J.S., 2016. Multiyear drought–induced morbidity preceding tree death in Southeastern US forests. Ecol. Appl. 26 (1), 17–23.

Bovard, B.D., Curtis, P.S., Vogel, C.S., Su, H.B., Schmid, H.P., 2005. Environmental controls on sap flow in a northern hardwood forest. Tree Physiol. 25 (1), 31–38.

Cai, G.H., Vanderborght, J., Langensiepen, M., Schnepf, A., Hueging, H., 2018. Root growth, water uptake, and sap flow of winter wheat in response to different soil water conditions. Hydrol. Earth Syst. Sci. 22 (4), 2449–2470.

Carrière, S.D., Martin-StPaul, N.K., Cakpo, C.B., Patris, N., Gillon, M., Chalikakis, K., Doussan, C., Olioso, A., Babic, M., Jouineau, A., Simioni, G., Davi, H., 2020. The role of deep vadose zone water in tree transpiration during drought periods in karst settings–insights from isotopic tracing and leaf water potential. Sci. Total Environ. 699, 134332.

Chen, H.S., Hu, K., Nie, Y.P., Wang, K.L., 2017. Analysis of soil water movement inside a footslope and a depression in a karst catchment. Southwest China. Sci. Rep. 7 (1), 1–13.

Clausnitzer, F., KoStner, B., Kai, S., Bernhofer, C., 2011. Relationships between canopy transpiration, atmospheric conditions and soil water availability—analyses of long–term sap–flow measurements in an old Norway spruce forest at the Ore Mountains/Germany. Agric. For. Meteorol. 151 (18), 1023–1034.

Deng, Y., Wu, S., Ke, J., Zhu, A.J., 2021. Effects of meteorological factors and groundwater depths on plant sap flow velocities in karst critical zone. Sci. Total Environ. 781, 146764.

Denissen, J.M.C., Teuling, A.J., Pitman, A.J., Koirala, S., Migliavacca, M., Li, W.T., Reichstein, M., Winkler, A.J., Zhan, C.H., Orth, R., 2022. Widespread shift from ecosystem energy to water limitation with climate change. Nat. Clim. Chang. 12 (7), 677–684.

Devi, H.M., Singh, N.I., 2018. Traditional medicinal uses and pharmacological properties of *Rhus chinensis* Mill.: a systematic review. Eur. J. Integr. Med. 21, 43–49.

Du, H., Liu, L., Su, L., Zeng, F.P., Wang, K.L., Peng, W.X., Zhang, H., Song, T.Q., 2019. Seasonal changes and vertical distribution of fine root biomass during vegetation restoration in a karst area, southwest China. Front. Plant Sci. 9, 2001.

Du, H., Zeng, F.P., Song, T.Q., Liu, K.P., Wang, K.L., Liu, M.X., 2021. Water depletion of climax forests over humid karst terrain: patterns, controlling factors and implications. Agr. Water Manage. 244, 106541.

Dudley, B.D., Marttila, H., Graham, S.L., Evison, R., Srinivasan, M.S., 2018. Water sources for woody shrubs on hillslopes: an investigation using isotopic and sapflow methods. Ecohydrology. 11 (2), e1926.

Dymond, S.F., Bradford, J.B., Bolstad, P.V., Kolka, R.K., Sebestyen, S.D., DeSutter, T.M., 2017. Topographic, edaphic, and vegetative controls on plant–available water. Ecohydrology. 10 (8), e1897.

Ellsworth, P.Z., Sternberg, L.S.L., 2015. Seasonal water use by deciduous and evergreen woody species in a scrub community is based on water availability and root distribution. Ecohydrology. 8 (4), 538–551.

Evaristo, J., Jasechko, S., Mcdonnell, J.J., 2015. Global separation of plant transpiration from groundwater and streamflow. Nature. 525 (7567), 91–94.

Fabiani, G., Schoppach, R., Penna, D., Klaus, J., 2021. Transpiration patterns and water use strategies of beech and oak trees along a hillslope. Ecohydrology. 15 (2), e2382.

Fan, Y., Clark, M., Lawrence, D.M., Swenson, S., Band, L.E., Brantley, S.L., Brooks, P.D., Dietrich, W.E., Flores, A., Grant, G., Kirchner, J.W., Mackay, D.S., McDonnell, J.J., Milly, P.C.D., Sullivan, P.L., Tague, C., Ajami, H., Chaney, N., Hartmann, A., Hazenberg, P., McNamara, J., Pelletier, J., Perket, J., Rouholahnejad-Freund, E., Wagener, T., Zeng, X., Beighley, E., Buzan, J., Huang, M., Livneh, B., Mohanty, B.P., Nijssen, B., Safeeq, M., Shen, C., van Verseveld, W., Volk, J., Yamazaki, D., 2019. Hillslope hydrology in global change research and earth system modeling. Water Resour. Res. 55 (2), 1737–1772.

Fu, Z.Y., Chen, H.S., Zhang, W., Xu, Q.X., Wang, S., Wang, K.L., 2015. Subsurface flow in a soil–mantled subtropical dolomite karst slope: a field rainfall simulation study. Geomorphology. 250, 1–14.

Gaj, M., Beyer, M., Koeniger, P., Wanke, H., Himmelsbach, T., 2015. In–situ unsaturated zone stable water isotope (^{2}H and ^{18}O) measurements in semi–arid environments using tunable off–axis integrated cavity output spectroscopy. Hydrol. Earth Syst. Sci. 12, 6115–6149.

Gessler, A., Bächli, L., Rouholahnejad Freund, E., Treydte, K., Schaub, M., Haeni, M., Weiler, M., Seeger, S., Marshall, J., Hug, C., Zweifel, R., Hagedorn, F., Rigling, A., Saurer, M., Meusburger, K., 2022. Drought reduces water uptake in beech from the drying topsoil, but no compensatory uptake occurs from deeper soil layers. New Phytol. 233 (1), 194–206.

Granier, A., 1987. Evaluation of transpiration in a Douglas-fir stand by means of sap flow measurements. Tree Physiol. 3, 309–320.

Gutierrez Lopez, J., Tor-Ngern, P., Oren, R., Kozii, N., Laudon, H., Hasselquist, N.J., 2021. How tree species, tree size, and topographical location influenced tree transpiration in northern boreal forests during the historic 2018 drought. Glob. Chang. Biol. 27 (13), 3066–3078.

Hawthorne, S., Miniat, C.F., 2017. Topography may mitigate drought effects on vegetation along a hillslope gradient. Ecohydrology 11 (1), e1825.

Hayat, M., Zha, T.S., Jia, X., Iqbala, S., Qian, D., Bourque, C.P.A., Khan, A., Tian, Y., Bai, Y.J., Liu, P., Yang, R.Z., 2020. A multiple–temporal scale analysis of biophysical control of sap flow in Salix psammophila growing in a semiarid shrubland ecosystem of northwest China. Agric. For. Meteorol. 288, 107985.

Heilman, J.L., Litvak, M.E., McInnes, K.J., Kjelgaard, J.F., Kamps, R.H., Schwinning, S., 2014. Water-storage capacity controls energy partitioning and water use in karst ecosystems on the Edwards Plateau. Texas. Ecohydrology. 7 (1), 127–138.

Huang, Y.Q., Zhao, P., Zhang, Z.F., Li, X.K., He, C.X., Zhang, R.Q., 2009. Transpiration of Cyclobalanopsis glauca (syn. *Quercus glauca*) stand measured by sap–flow method in a karst rocky terrain during dry season. Ecol. Res. 24 (4), 791–801.

Huang, K.C., Wang, Q., Otieno, D., 2021. Responses of sap flux densities of different plant functional types to environmental variables are similar in both dry and wet seasons in a subtropical mixed forest. Forests. 12 (8), 1007.

Huang, L., Lian, J.J., Nie, Y.P., Ma, X.Y., Liu, W.N., Wang, Z.Y., Chen, H.S., 2022. Selective removal of non–woody species released water limitation on vegetation community stagnated at early successional stages in a humid karst region. J. Hydrol. 615, 128714.

Jasechko, S., Sharp, Z.D., Gibson, J.J., Birks, S.J., Yi, Y., Fawcett, P.J., 2013. Terrestrial water fluxes dominated by transpiration. Nature. 496 (7445), 347–350.

Jencso, K.G., McGlynn, B.L., Gooseff, M.N., Wondzell, S.M., Bencala, K.E., Marshall, L.A., 2009. Hydrologic connectivity between landscapes and streams: transferring reach–and plot–scale understanding to the catchment scale. Water Resour. Res. 45 (4).

Jiang, Z.C., Lian, Y.Q., Qin, X.Q., 2014. Rocky desertification in Southwest China: impacts, causes, and restoration. Earth–Sci. Rev. 132, 1–12.

Jiao, L., Lu, N., Fang, W.W., Li, Z.S., Wang, J., Jin, Z., 2019. Determining the independent impact of soil water on forest transpiration: a case study of a black locust plantation in the Loess Plateau. China. J. Hydrol. 572, 671–681.
Juhlke, T.R., Van Geldern, R., Barth, J.A.C., Bendix, J., Brauning, A., Garel, E., Hausser, M., Huneau, F., Knerr, I., Santoni, S., Szymczak, S., Trachte, K., 2021. Temporal offset between precipitation and water uptake of Mediterranean pine trees varies with elevation and season. Sci. Total Environ. 755, 142539.
Kumagai, T., Aoki, S., Shimizu, T., Otsuki, K., 2007. Sap flow estimates of stand transpiration at two slope positions in a Japanese cedar forest watershed. Tree Physiol. 27 (2), 161–168.
Landwehr, J.M., Coplen, T.B., 2006. Line–conditioned excess: a new method for characterizing stable hydrogen and oxygen isotoperatios in hydrologic systems. International Conference on Isotopes in Environmental Studies. IAEA, Vienna, pp. 132–135.
Liu, H.Y., Jiang, Z.H., Dai, J.X., Wu, X.C., Peng, J., Wang, H.Y., Meersmans, J., Green, S.M., Quine, T.A., 2019. Rock crevices determine woody and herbaceous plant cover in the karst critical zone. Sci. China Earth Sci. 62 (11), 1756–1763.
Liu, W.N., Chen, H.S., Zou, Q.Y., Nie, Y.P., 2021. Divergent root water uptake depth and coordinated hydraulic traits among typical karst plantations of subtropical China: implication for plant water adaptation under precipitation changes. Agr. Water Manage. 249, 106798.
Liu, Z.Q., Wei, Z.J., Jiang, J., Yu, X.X., 2022. Adaptability of tree water use to elevation changes: a case study of a mixed forest in Northern China. J. Hydrol. 613, 128407.
Liu, Z., Ye, L., Jiang, J., Liu, R., Xu, Y., Jia, G., 2023. Increased uptake of deep soil water promotes drought resistance in mixed forests. Plant Cell Environ., 1–11 https://doi.org/10.1111/pce.14642.
Looker, N., Martin, J., Hoylman, Z., Jencso, K., Hu, J., 2018. Diurnal and seasonal coupling of conifer sap flow and vapour pressure deficit across topoclimatic gradients in a subalpine catchment. Ecohydrology 11 (7), e1994.
Loranty, M.M., Mackay, D.S., Ewers, B.E., Adelman, J.D., Kruger, E.L., 2008. Environmental drivers of spatial variation in whole–tree transpiration in an aspen–dominated upland–to–wetland forest gradient. Water Resour. Res. 44 (2), W02441.
Luo, Z.D., Nie, Y.P., Chen, H.S., Guan, H.D., Zhang, X.P., Wang, K.L., 2023. Water age dynamics in plant transpiration: the effects of climate patterns and rooting depth. Water Resour. Res. https://doi.org/10.1029/2022WR033566.
Ma, X.Y., Chen, H.S., Nie, Y.P., 2020. Common species maintain a large root radial extent and a stable resource use status in soil–limited environments: a case study in subtropical China. Front. Plant Sci. 11, 1260.
Meng, Q.M., Wang, S., Fu, Z.Y., Deng, Y.S., Chen, H.S., 2022. Soil types determine vegetation communities along a toposequence in a dolomite peak–cluster depression catchment. Plant Soil 475, 5–22.
Mitchell, P.J., Benyon, R.G., Lane, P.N., 2012. Responses of evapotranspiration at different topographic positions and catchment water balance following a pronounced drought in a mixed species eucalypt forest. Australia. J. Hydrol. 440, 62–74.
Mohanty, B.P., Mousli, Z., 2000. Saturated hydraulic conductivity and soil water retention properties across a soil–slope transition. Water Resour. Res. 36 (11), 3311–3324.
Naithani, K.J., Ewers, B.E., Pendall, E., 2012. Sap flux–scaled transpiration and stomatal conductance response to soil and atmospheric drought in a semi–arid sagebrush ecosystem. J. Hydrol. 464, 176–185.
Nathaniel, L., Justin, M., Zachary, H., Kelsey, J., Jia, H., 2018. Diurnal and seasonal coupling of conifer sap flow and vapor pressure deficit across topoclimatic gradients in a subalpine catchment. Ecohydrology e1994.
Nie, Y.P., Chen, H.S., Wang, K.L., Ding, Y.L., 2014. Rooting characteristics of two widely distributed woody plant species growing in different karst habitats of southwest China. Plant Ecol. 215 (10), 1099–1109.
Nie, Y., Chen, H., Ding, Y., Wang, K., Pugnaire, F., 2018. Water source segregation along successional stages in a degraded karst region of subtropical China. J. Veg. Sci. 29, 933–942.
Nie, Y.P., Ding, Y.L., Zhang, H.L., Chen, H.S., 2019. Comparison of woody species composition between rocky outcrops and nearby matrix vegetation on degraded karst hillslopes of Southwest China. J. Forestry Res. 30 (3), 911–920.
North, L.A., Van Beynen, P.E., Parise, M., 2009. Interregional comparison of karst disturbance: West–central Florida and southeast Italy. J. Environ. Manag. 90 (5), 1770–1781.
Novick, K.A., Ficklin, D.L., Stoy, P.C., Williams, C.A., Bohrer, G., Oishi, A.C., Papuga, S.A., Blanken, P.D., Noormets, A., Sulman, B.N., Scott, R.L., Wang, L.X., Phillips, R.P., 2016. The increasing importance of atmospheric demand for ecosystem water and carbon fluxes. Nat. Clim. Chang. 6 (11), 10213–11027.
Oogathoo, S., Houle, D., Duchesne, L., Kneeshaw, D., 2020. Vapour pressure deficit and solar radiation are the major drivers of transpiration of balsam fir and black spruce tree species in humid boreal regions, even during a short–term drought. Agric. For. Meteorol. 291, 108063.
Pacific, V.J., McGlynn, B.L., Riveros–Iregui, D.A., Welsch, D.L., Epstein, H.E., 2011. Landscape structure, groundwater dynamics, and soil water content influence soil respiration across riparian–hillslope transitions in the Tenderfoot Creek Experimental Forest, Montana. Hydrol. Process. 25 (5), 811–827.
Pei, Z., Hao, S., Pang, G., Wang, K., Liu, T., 2019. Sap flow of salix psammophila and its principal influencing factors at different slope positions in the mu us desert. PLoS ONE 14 (12), e0225653.
Renner, M., Hassler, S.K., Blume, T., Weiler, M., Hildebrandt, A., Guderle, M., Schymanski, S.J., Kleidon, A., 2016. Dominant controls of transpiration along a hillslope transect inferred from ecohydrological measurements and thermodynamic limits. Hydrol. Earth Syst. Sci. 20 (5), 2063–2083.
Schlesinger, W.H., Jasechko, S., 2014. Transpiration in the global water cycle. Agric. For. Meteorol. 189, 115–117.
Schultz, N.M., Griffis, T.J., Lee, X.H., Baker, J.M., 2011. Identification and correction of spectral contamination in 2H/1H and $^{18}O/^{16}O$ measured in leaf, stem, and soil water. Rapid Commun Mass Sp. 25 (21), 3360–3368.
Schwinning, S., 2010. The ecohydrology of roots in rocks. Ecohydrology. 3 (2), 238–245.
Song, X.F., Wang, S.Q., Xiao, G.Q., Wang, Z.M., Liu, X., Wang, P., 2009. A study of soil water movement combining soil water potential with stable isotopes at two sites of shallow groundwater areas in the North China Plain. Hydrol. Process. 23 (9), 1376–1388.
Song, X.W., Lyu, S.D., Wen, X.F., 2020. Limitation of soil moisture on the response of transpiration to vapor pressure deficit in a subtropical coniferous plantation subjected to seasonal drought. J. Hydrol. 591, 125301.
Tong, X.W., Brandt, M., Yue, Y.M., Horion, S., Wang, K.L., De Keersmaecker, W., Tian, F., Schurgers, G., Xiao, X.M., Luo, Y.Q., Chen, C., Myneni, R., Shi, Z., Chen, H.S., Fensholt, R., 2018. Increased vegetation growth and carbon stock in China karst via ecological engineering. Nat. Sustain. 1, 44–50.
Tsuruta, K., Yamamoto, H., Kosugi, Y., Makita, N., Katsuyama, M., Kosugi, K.I., Tani, M., 2020. Slope position and water use by trees in a headwater catchment dominated by Japanese cypress: implications for catchment–scale transpiration estimates. Ecohydrology. 13 (8), e2245.
Ungar, E.D., Rotenberg, E., Raz-Yaseef, N., Cohen, S., Yakir, D., Schiller, G., 2013. Transpiration and annual water balance of Aleppo pine in a semiarid region: implications for forest management. For. Ecol. Manag. 298, 39–51.
Vose, J.M., Miniat, C.F., Luce, C.H., Asbjornsen, H., Caldwell, P.V., Campbell, J.L., 2016. Ecohydrological implications of drought for forests in the United States. For. Ecol. Manag. 380, 335–345.
Wang, H.L., Zheng, J.H., 2022. Assessing the effects of surface conditions on potential evapotranspiration in a humid subtropical region of China. Front. Clim. 4, 813787.
Wang, Y.B., Wang, Y.H., Xiong, W., Yao, Y.Q., Zhang, T., Li, Z.H., 2017. Variation in the sap flow velocity of Larix principis–rupprechtii and its impact factors in different slope positions in a semi–arid region of Liupan Mountains. Scientia Silvae Sinicae. 53 (6), 10–20.
Wang, K.L., Zhang, C.H., Chen, H.S., Yue, Y.M., Zhang, W., Zhang, M.Y., Qi, X.K., Fu, Z.Y., 2019. Karst landscapes of China: patterns, ecosystem processes and services. Landsc. Ecol. 34 (12), 2743–2763.
Wang, S., Fu, Z.Y., Chen, H.S., Nie, Y.P., Xu, Q.X., 2020. Mechanisms of surface and subsurface runoff generation in subtropical soil–epikarst systems: implications of rainfall simulation experiments on karst slope. J. Hydrol. 580, 124370.
Williams, P.W., 1983. The role of the subcutaneous zone in karst hydrology. J. Hydrol. 61 (1–3), 45–67.
Williams, P.W., 2008. The role of the epikarst in karst and cave hydrogeology: a review. Int. J. Speleol. 37 (1), 1–10.
Wu, H., Zhao, G., Li, X.Y., Wang, Y., Sun, W., 2019. Identifying water sources used by alpine riparian plants in a restoration zone on the Qinghai-Tibet plateau: evidence from stable isotopes. Sci. Total Environ. 697, 134092.
Wu, Z., Behzad, H.M., He, Q.F., Wu, C., Bai, Y., Jiang, Y.J., 2021. Seasonal transpiration dynamics of evergreen Ligustrum lucidum linked with water source and water–use strategy in a limestone karst area, southwest China. J. Hydrol. 597, 126199.
Xu, C.H., Xu, X.L., Liu, M.X., Li, Z.W., Zhang, Y.H., Zhu, J.X., Wang, K.L., Chen, X., Zhang, Z.C., Peng, T., 2020. An improved optimization scheme for representing hillslopes and depressions in karst hydrology. Water Resour. Res. 56 (5) e2019WR026038.
Yan, Y.J., Dai, Q.H., Yang, Y.Q., Yan, L.B., Yi, X.S., 2022. Epikarst shallow fissure soil systems are key to eliminating karst drought limitations in the karst rocky desertification area of SW China. Ecohydrology. 15 (2), e2372.
Yang, J., Chen, H.S., Nie, Y.P., Wang, K.L., 2019. Dynamic variations in profile soil water on karst hillslopes in Southwest China. Catena. 172, 655–663.
Yang, Q., Liu, G., Xu, L., Ulgiati, S., Casazza, M., Hao, Y., Lu, Z.M., Deng, X.Y., Yang, Z., 2022. Hidden challenges behind ecosystem services improvement claims. Iscience. 25 (9), 104928.
Yin, Q.C., 2011. Research on photosynthetically and ecophysiological characteristic of typical plants in karst area, northwest Guangxi. Nanning, Guangxi University 11–13 (in Chinese).
Yuan, D.X., Zhu, D.H., Weng, J.T., 1994. Karstology of China. Geological Publishing House, Beijing, China (in Chinese).
Zeng, X.M., Xu, X.L., Yi, R.Z., Zhong, F.X., Zhang, Y.H., 2021. Sap flow and plant water sources for typical vegetation in a subtropical humid karst area of southwest China. Hydrol. Process. 35 (3), e14090.
Zhang, R.F., Xu, X.L., Liu, M.X., Zhang, Y.H., Xu, C.H., Yi, R.Z., Luo, W., Soulsby, C., 2019a. Hysteresis in sap flow and its controlling mechanisms for a deciduous broad–leaved tree species in a humid karst region. Sci. China Earth Sci. 62 (11), 1744–1755.
Zhang, Z.C., Chen, X., Cheng, Q.B., Soulsby, C., 2019b. Storage dynamics, hydrological connectivity and flux ages in a karst catchment: conceptual modelling using stable isotopes. Hydrol. Earth Syst. Sc. 23 (1), 51–71.
Zhang, X., Zhao, W.W., Wang, L.X., Liu, Y.X., Liu, Y., Qing, F., 2019c. Relationship between soil water content and soil particle size on typical slopes of the Loess Plateau during a drought year. Sci. Total Environ. 648, 943–954.
Zhang, J., Wang, S., Fu, Z.Y., Chen, H.S., Wang, K.L., 2022. Soil thickness controls the rainfall–runoff relationship at the karst hillslope critical zone in southwest China. J. Hydrol. 609, 127779.
Zhang, J., Chen, H., Fu, Z., Wang, F., Wang, K., 2023. Towards hydrological connectivity in the karst hillslope critical zone: insight from using water isotope signals. J. Hydrol. 617, 128926.
Zhou, C., Huang, M., Ren, H., Yu, J., Wu, J., Ma, X., 2017. Bioaccumulation and detoxification mechanisms for lead uptake identified in *Rhus chinensis* Mill. seedlings. Ecotox. Environ. Safe. 142, 59–68.
Zunzunegui, M., Boutaleb, S., Barradas, M.C.D., Esquivias, M.P., Valera, J., Jauregui, J., Tagma, T., Ain-Lhout, F., 2018. Reliance on deep soil water in the tree species argania spinosa. Tree Physiol. 38 (5), 678–689.